Contribution from the Department of Chemistry and Biochemistry, University of California, Los Angeles, California 90024

Substitution by Phosphorus Ligands on Edge-Double-Bridged Triruthenium Carbonyl Complexes and on $Ru_2\{\mu\text{-}O{=}C(Et)\}_2(CO)_6$: ^{13}C NMR Characterization

CARSTEN E. KAMPE and HERBERT D. KAESZ*

Received July 12, 1984

Edge-double-bridged triruthenium carbonyl complexes and a double-bridged dinuclear complex undergo facile substitution of a carbonyl group by a phosphorus ligand at 25 °C in hexane solution. When a bridging acyl group is present, substitution occurs exclusively on the ruthenium atom to which the acyl oxygen atom is bonded. The starting materials undergo rapid exchange with ^{13}CO, permitting their enrichment for ^{13}C NMR studies. The four systems studied are presented in their order of increasing reactivity. (1) The complex $Ru_3\{\mu\text{-}H,\mu\text{-}O{=}C(Me)\}(CO)_{10}$ reacts within 4 h with 1 molar equiv of triphenylphosphine to give the substitution product $Ru_3\{\mu\text{-}H,\mu\text{-}O{=}C(Me)\}(CO)_9PPh_3$ in 48% yield. Starting material (25%) and some 10% of the complex $Ru_3(CO)_{11}PPh_3$ are also obtained. With excess triphenylphosphine less of the monosubstituted acyl hydrido complex is obtained. Reaction with $P(OMe)_3$ requires an excess of phosphite, but then only a 15% yield of $Ru_3\{\mu\text{-}H,\mu\text{-}O{=}C(Me)\}(CO)_9P(OMe)_3$ is isolated along with $Ru_3(CO)_{11}P(OMe)_3$ (5%). (2) The complexes $Ru_3\{\mu\text{-}H,\mu\text{-}X\}(CO)_{10}$ react within 10 min with 1 equiv of triphenylphosphine to yield the products $Ru_3\{\mu\text{-}H,\mu\text{-}X\}(CO)_9PPh_3$, X = Cl, Br, I, respectively. When X = I, a carbonyl group is readily lost from the product to give $Ru_3\{\mu\text{-}H,\mu_3\text{-}I\}(CO)_8PPh_3$. This transformation is reversible. Variable-temperature ^{13}C NMR study of $Ru_3\{\mu\text{-}H,\mu\text{-}Cl\}(CO)_9PPh_3$ and $Ru_3\{\mu\text{-}H,\mu\text{-}Br\}(CO)_9PPh_3$ indicates an intramolecular polytopal rearrangement for the three carbonyl groups of the $Ru(CO)_3$ unit on the bridged edge: coalescence temperature −45 °C. (3) The complexes $Ru_3\{\mu\text{-}X,\mu\text{-}O{=}C(Et)\}(CO)_{10}$, X = Cl, Br, I, react in less than 1 min with triphenylphosphine to give nearly quantitative yields of $Ru_3\{\mu\text{-}X,\mu\text{-}O{=}C(Et)\}(CO)_9PPh_3$ (98, 95, and 93%, respectively) or trimethyl phosphite to give $Ru_3\{\mu\text{-}X,\mu\text{-}O{=}C(Et)\}(CO)_9P(OMe)_3$ (78, 75, and 68%, respectively). Exposure of $Ru_3\{\mu\text{-}Cl,\mu\text{-}O{=}C(Et)\}(CO)_{10}$ in chloroform solution to an atmosphere of ^{13}CO leads to initial enrichment at six sites; the enrichment equilibrates with the remaining four carbonyl groups over a period of 8 h. (4) The dinuclear complex $Ru_2\{\mu\text{-}O{=}C(Et)\}_2(CO)_6$ reacts in less than 1 min with phosphorus ligands to give quantitative yields of the monosubstituted derivative $(CO)_2(L)Ru\{\mu\text{-}O{=}C(Et)\}_2Ru(CO)_3$, L = PPh_3, $P(OMe)_3$, $P(OPh)_3$. Exposure of $Ru_2\{\mu\text{-}O{=}C(Et)\}_2(CO)_6$ in chloroform solution to an atmosphere of ^{13}CO leads to instantaneous specific enrichment at three sites on the ruthenium atom bonded to the acyl oxygen atoms, equilibrating to the remaining three sites in 8 h.

Introduction

As described in the immediately preceding paper,[1] earlier attempts to prepare derivatives of the anion $[Ru_3\{\mu\text{-}O{=}CNMe_2\}\{\mu\text{-}CO\}_3(CO)_7^-]$ led us to observe a remarkably rapid substitution with trialkyl or triaryl phosphite ligands. In this paper the reaction of phosphorus ligands with a variety of newly isolated neutral complexes is reported: $Ru_3\{\mu\text{-}H,\mu\text{-}O{=}C(Me)\}(CO)_{10}$ (**4**),[2] $Ru_3\{\mu\text{-}H,\mu\text{-}X\}(CO)_{10}$, X = Cl (**1a**), Br (**1b**), I (**1c**),[3] $Ru_3\{\mu\text{-}X,\mu\text{-}O{=}C(Et)\}(CO)_{10}$, X = Cl (**6a**), Br (**6b**), I (**6c**),[4] and $Ru_2\{\mu\text{-}O{=}C(Et)\}_2(CO)_6$ (**8**).[4] We found a high reactivity toward substitution, which prompted us to enrich the starting materials with ^{13}CO. We here also report a ^{13}C NMR study of these edge-double-bridged di- and triruthenium complexes and their substituted derivatives.

Results

The transformations achieved in this study are summarized in Schemes I and II. Conditions for each of the reactions, the yield of each product isolated, and coupling constant data are also presented in these schemes. Structural assignments derived from these data are explained in the Discussion. Complete spectroscopic data are given in Tables I–IV.

^{13}C NMR. To facilitate ^{13}C NMR, all samples were enriched to approximately 30% ^{13}CO prior to the introduction of the phosphorus ligands. This was achieved by exposure of the starting materials in hexane solution to a calibrated volume of 99% ^{13}CO at 1 atm. Contact times of 1–5 min are found sufficient for the necessary enrichments, which in our experience are the most rapid exchanges yet reported for triruthenium cluster complexes; cf. 3-h time period for 50% completion for the ^{13}CO exchange in the anions $[Ru_3\{\mu\text{-}OC(R)O\}(CO)_{10}^-]$ (R = H, CH_3)[5] or for $Ru_3(CO)_{12}$ in the presence[6] of H^- (which has been attributed to exchange in the anion $[Ru_3\{\mu\text{-}H,\mu\text{-}CO\}(CO)_{10}^-]$).[5]

The ^{13}C NMR data for some of the starting complexes have been published, namely **1a–c**[3b] and **4**.[3a] Those for **1a** and **4**

Scheme I[a]

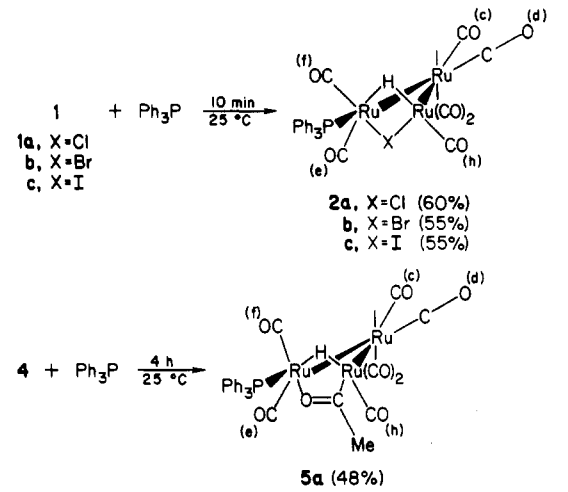

[a] Coupling constants are as follows (Hz): 2a, $J_{PH} = 5.4$, $J_{PCe} = 5.9$, $J_{CeH} = 11.0$, $J_{PCf} = 5.9$, $J_{ChH} = 15.9$, $^3J_{PCd} = 11.6$; 5a, $J_{PH} = 9.6$, $J_{PCe} = 5.3$, $J_{CeH} = 14.1$, $J_{PCf} = 7.0$, $J_{ChH} = 12.3$, $^3J_{PCd} = 12.3$.

(1) Mayr, A.; Lin, Y. C.; Boag, N. M.; Kampe, C. E.; Knobler, C. B.; Kaesz, H. D. *Inorg. Chem.*, preceding paper in this issue.
(2) Mayr, A.; Lin, Y. C.; Boag, N. M.; Kaesz, H. D. *Inorg. Chem.* **1982**, *21*, 1704.
(3) (a) Preliminary Communication: Boag, N. M.; Kampe, C. E.; Lin, Y. C.; Kaesz, H. D. *Inorg. Chem.* **1982**, *21*, 1706. (b) Full paper: Kampe, C. E.; Boag, N. M.; Knobler, C. B.; Kaesz, H. D. *Inorg. Chem.* **1984**, *23*, 1390–1397.
(4) (a) Preliminary communication: Kampe, C. E.; Boag, N. M.; Kaesz, H. D. *J. Am. Chem. Soc.* **1983**, *105*, 2896. (b) Full paper: Kampe, C. E.; Boag, N. M.; Kaesz, H. D. *J. Mol. Catal.* **1983**, *21*, 279–291.
(5) Darensbourg, D. J.; Pala, M.; Waller, J. *Organometallics* **1983**, *2*, 1285–1291.
(6) Bricker, J. C.; Nagel, C. C.; Shore, S. G. *J. Am. Chem. Soc.* **1982**, *104*, 1444–1445.

0020-1669/84/1323-4646$01.50/0

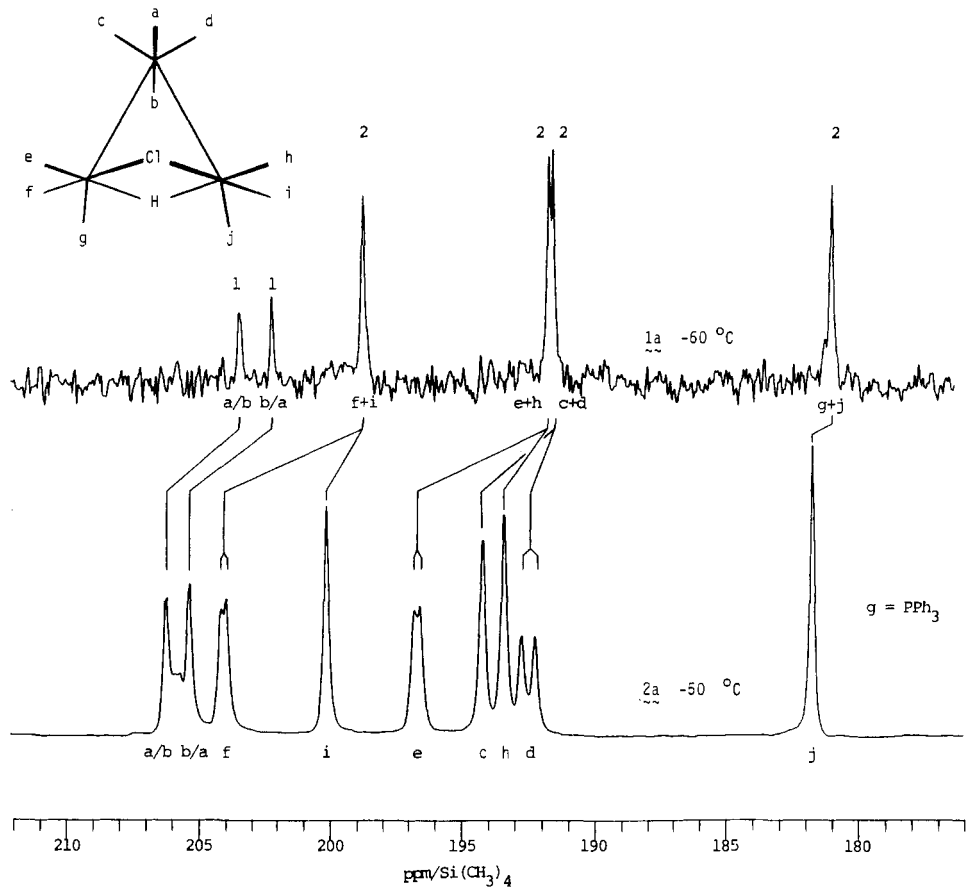

Figure 1. $^{13}C\{^1H\}$ NMR spectra in the carbonyl region for ^{13}CO-enriched compounds ($CDCl_3$ solution with $Cr(acac)_3$ (0.05 M)): (upper trace) $Ru_3\{\mu\text{-}H,\mu\text{-}Cl\}(CO)_{10}$ (**1a**), −60 °C; (lower trace) $Ru_3\{\mu\text{-}H,\mu\text{-}Cl\}(CO)_9PPh_3$ (**2a**), −50 °C.

Scheme II[a]

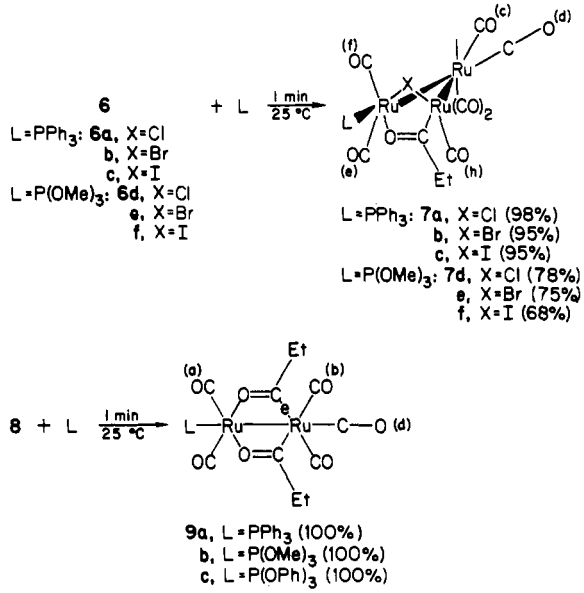

[a] Coupling constants are as follows (Hz): 7a, $J_{PCe} = 5.3$, $J_{PCf} = 3.5$, $^3J_{PCd} = 17.6$; 9b, $J_{PCa} = 7.0$, $^3J_{PCb} = 3.5$, $J_{PCd} = 29.9$, $^3J_{PCe} = 3.5$.

Table I. IR Data (Hexane)

compd	ν(CO), cm^{-1}	ν(C=O), cm^{-1}
2a	2094 m, 2060 s, 2025 sh, 2016 vs, 1988 w, 1965 w	
2b	2094 m, 2056 s, 2024 sh, 2016 vs, 1988 w, 1964 w	
2c	2092 m, 2059 s, 2021 vs, 2014 sh, 1988 w, 1956 w	
3	2076 m, 2043 vs, 2017 s, 2000 s, 1979 w, 1973 vw	
5a	2086 s, 2047 vs, 2019 s, 2015 sh, 2006 m, 1993 m, 1978 w, 1960 w	1524
5b	2089 s, 2049 vs, 2027 s, 2022 s, 2016 s, 2006 s, 1994 m, 1979 w	1519
7a	2088 s, 2054 vs, 2021 m, 2015 m, 2008 sh, 1996 s, 1989 sh, 1975 w, 1957 w	1526
7b	2087 s, 2053 vs, 2020 m, 2013 m, 2008 sh, 1997 s, 1988 sh, 1974 w, 1956 w	1526
7c	2086 s, 2052 vs, 2018 m, 2012 sh, 2008 m, 1997 s, 1988 sh, 1977 w, 1954 w	1522
7d	2089 m, 2059 vs, 2027 sh, 2020 s, 2005 m, 1995 s, 1975 w	1521
7e	2089 m, 2055 vs, 2026 sh, 2020 s, 2006 m, 1996 s, 1976 w	1520
7f	2087 m, 2053 vs, 2025 sh, 2018 s, 2007 m, 1997 s, 1981 w	1518
9a	2056 vs, 2005 s, 1968 m, 1946 w	1529
9b	2059 vs, 2012 sh, 2004 s, 1969 s, 1960 m	1523
9c	2062 vs, 2014 sh, 2008 s, 1973 s, 1966 sh	1528

are repeated in Table III to compare with data for the other complexes. Data for **8** are presented in Table IV.

Low-temperature ^{13}C NMR spectra for the carbonyl region of **1a** and **2a** are shown in Figure 1. The room-temperature spectrum for **2a** is shown in Figure 2 (top scan); resonances h, i, and j, associated with carbonyl groups undergoing rapid exchange at this temperature, are absent. A proton-coupled low-temperature spectrum of **2a** is shown in the lower scan of Figure 2.

Room-temperature spectra for **4** and its triphenylphosphine-substituted derivative, **5a**, are presented in Figure 3. These complexes undergo no fluxional processes at this temperature; their spectra assist in making assignments of

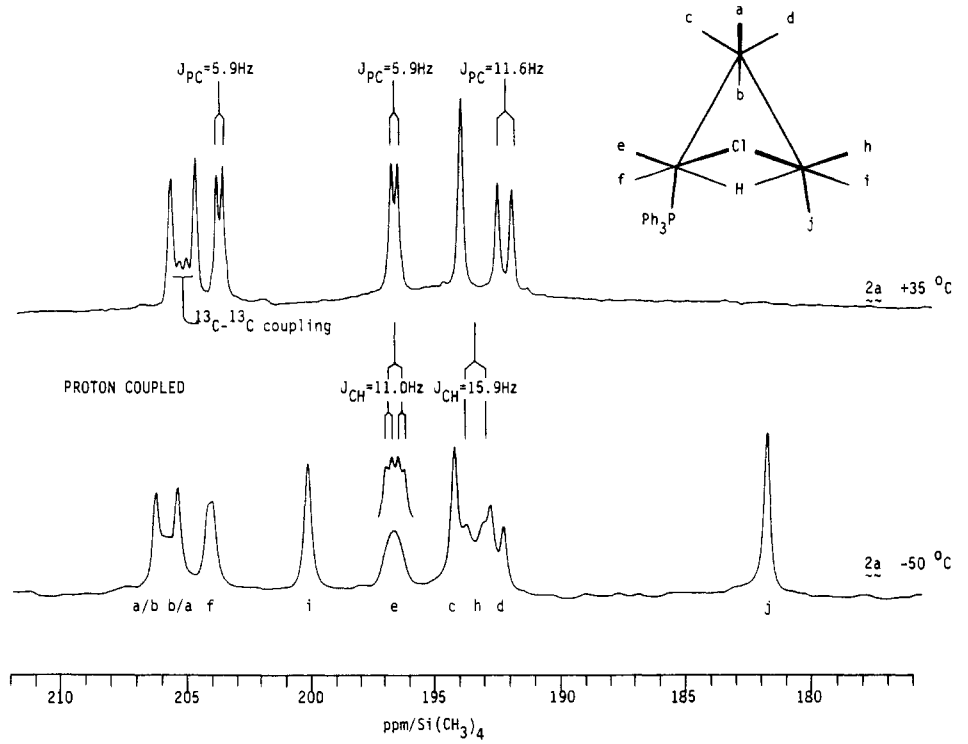

Figure 2. ^{13}C NMR spectra in the carbonyl region for $Ru_3\{\mu\text{-}H,\mu\text{-}Cl\}(CO)_9PPh_3$ (**2a**) (^{13}CO enriched, $CDCl_3$ solution with $Cr(acac)_3$ (0.05 M)): (upper trace) proton decoupled, 35 °C; (lower trace) proton coupled, −50 °C.

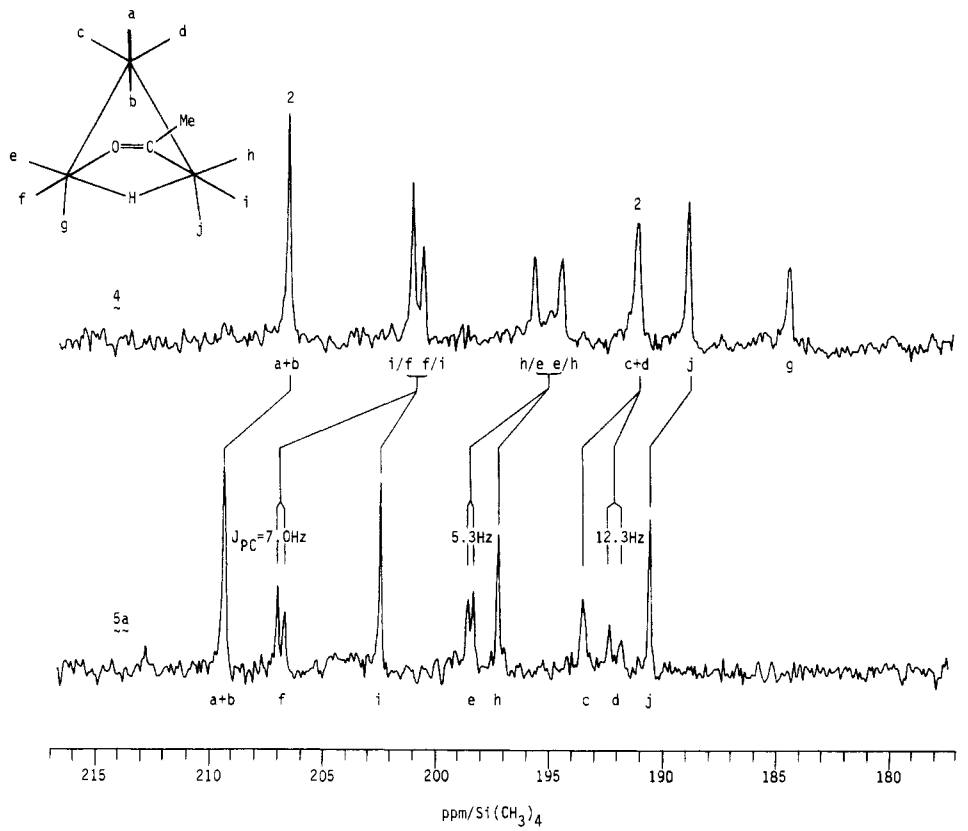

Figure 3. $^{13}C\{^1H\}$ NMR spectra in the carbonyl region for ^{13}CO-enriched compounds ($CDCl_3$ solution with $Cr(acac)_3$ (0.05 M), 25 °C): (upper trace) $Ru_3\{\mu\text{-}H,\mu\text{-}O{=}CMe\}(CO)_{10}$ (**4**); (lower trace) $Ru_3\{\mu\text{-}H,\mu\text{-}O{=}CMe\}(CO)_9PPh_3$ (**5a**).

resonances. The spectra of **6a** and **7a** are also useful in this respect and are offered as Figure 4 (supplementary material). Room-temperature spectra for $Ru_2\{\mu\text{-}O{=}C(Et)\}_2(CO)_6$ (**8**) and its trimethyl phosphite substituted derivative, **9b**, are presented in Figure 5. Assignment of the resonances is presented in the Discussion.

Site-Specific ^{13}CO Enrichment in $Ru_3\{\mu\text{-}Cl,\mu\text{-}O{=}C(Et)\}(CO)_{10}$ (6a) and $Ru_2\{\mu\text{-}O{=}C(Et)\}_2(CO)_6$ (8). Samples of **6a** and **8** in $CDCl_3$ were each exposed to 1 atm of ^{13}CO (99%) for 0.5 h, after which the gases were displaced with N_2. Enrichment was followed over an 8-h period with spectra taken at 0.5-h intervals. The area under each of the peaks was

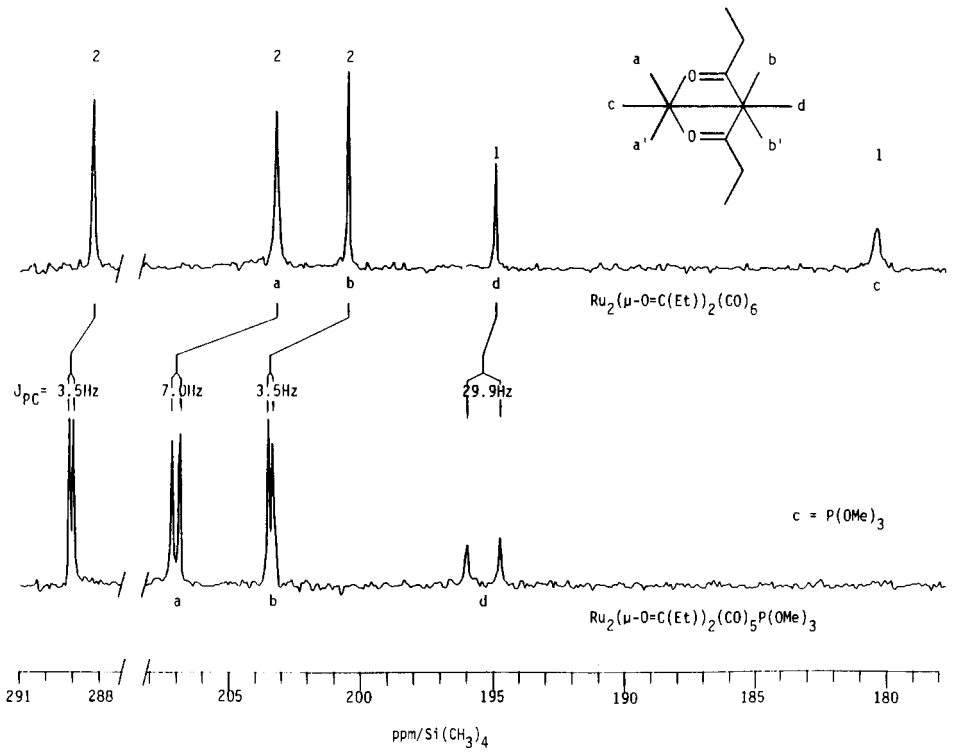

Figure 5. $^{13}C\{^1H\}$ NMR spectra in the carbonyl region for ^{13}CO-enriched compounds ($CDCl_3$ solution with $Cr(acac)_3$ (0.05 M), 25 °C): (upper trace) $Ru_2(\mu\text{-}O{=}CEt)_2(CO)_6$ (**8**); (lower trace) $Ru_2\{\mu\text{-}O{=}CEt\}_2(CO)_5P(OMe)_3$ (**9b**).

Table II. ^{31}P and ^1H NMR Data[a]

compd	^{31}P[b]	^1H[c]
2a	28.7	7.2-7.5 (m, C_6H_5); −13.0 (1, RuHRu, d, J_{PH} = 5.42)
2b	30.8	7.2-7.5 (m, C_6H_5); −13.5 (1, RuHRu, d, J_{PH} = 5.30)
2c	31.4	7.2-7.5 (m, C_6H_4); −14.3 (1, RuHRu, d, J_{PH} = 4.80)
3	31.9	7.2-7.5 (m, C_6H_5); −16.1 (1, RuHRu, d, J_{PH} = 10.3)
5a	37.5	7.4-7.5 (m, C_6H_5); 2.12 (s, CH_3), −13.50 (1, RuHRu, d, J_{PH} = 9.61)
7a	22.7	7.3-7.5 (m, C_6H_5); 3.07 (δ_A), 2.67 (δ_B) (CH_2, J_{AB} = 18.31, J_{AH} = J_{BH} = 7.08); 0.611 (CH_3, J = 7.08)
7b	21.9	7.3-7.5 (m, C_6H_5); 3.07 (δ_A), 2.63 (δ_B) (CH_2, J_{AB} = 18.31, J_{AH} = J_{BH} = 7.08); 0.578 (CH_3, J = 7.08)
7c	21.1	7.3-7.5 (m, C_6H_5); 3.01 (δ_A), 2.52 (δ_B) (CH_2, J_{AB} = 18.01, J_{AH} = J_{BH} = 7.08); 0.522 (CH_3, J = 7.08)
7d	153	3.10 (2, q, CH_2); 1.02 (3, t, J = 7.08, CH_3); 3.77 (9, d, J_{PH} = 11.4)
7e	152	3.07 (2, q, CH_2); 0.98 (3, t, J = 7.08, CH_3); 3.77 (9, d, J_{PH} = 11.5)
7f	151	2.97 (2, q, CH_2); 0.89 (3, t, J = 7.08, CH_3); 3.77 (9, d, J_{PH} = 11.7)
9a	14.3	7.2-7.7 (m, C_6H_5); 2.3-2.9 (m, CH_2, δ_A = 2.70, δ_B = 2.63, J_{AB} = 6.0, J_{AH} = 7.03, J_{BH} = 7.32 Hz); 0.791 (t, CH_3, J = 7.18)
9b	131	3.85 (9, d, J_{PH} = 12.0); 2.68 (ABX_3); 0.918 (3, t, J = 7.32)
9c	116	6.8-7.5 (15, $-OC_6H_5$)

[a] Solvent $CDCl_3$; coupling constants in Hz. [b] In ppm relative to H_3PO_4. [c] In ppm relative to Me_4Si.

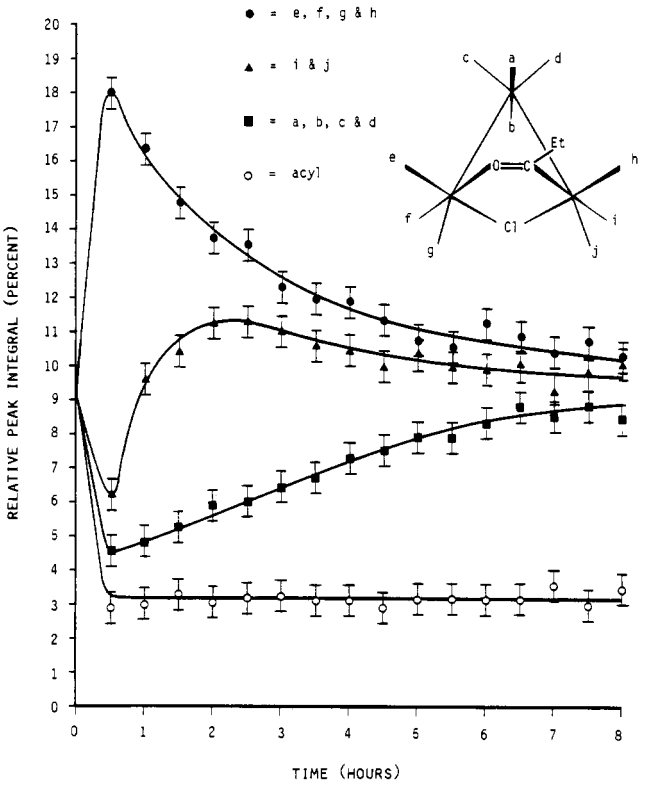

Figure 6. Site-specific enrichment in **6a** and internal equilibration throughout the population of terminally bonded carbonyl groups. Signals for the individual resonances have been normalized to the same relative peak integral in the spectrum at natural ^{13}C abundance; see text for further details.

measured for a sample at natural abundance and normalized to represent an individual carbonyl group, as relative percent of the total signal area. The results for each of these two derivatives are presented in Figures 6 and 7. The initial points (at time = 0) thus show all carbonyl groups to be represented at equal relative intensity in both figures. The spectra at natural ^{13}C abundance as well as spectra after the initial exposure and after 8 h of internal equilibration are presented in Figures 8 and 9 (supplementary material).

In **6a** specific ^{13}C enrichment is observed initially for four resonances, e, f, g, and h. The enrichment quickly equilibrates into two other carbonyl groups, i and j, and more slowly into

Table III. ^{13}C NMR Data[a,b]

compd	O=C(R)	CO[d]	other
1a		203.2, 202.0, 198.7 (2),* 191.7 (2),* 191.5 (2), 181.0 (2)*	
2a		205.1, 204.8, 203.9 (*d*, J_{PC} = 5.9), 200.0,* 196.6 (dd, J_{PC} = 5.9, J_{CH} = 11.0), 194.1, 193.3,* 192.4 (dd, J_{PC} = 11.6, J_{CH} = 15.9), 181.8*	128-134 (m, Ph)
2b		207.1, 206.4, 203.6 (d, J_{PC} = 6.1), 199.7,* 196.5 (d, J_{PC} = 6.1), 193.9, 192.9,* 192.2 (d, J_{PC} = 11.0), 182.1*	128-134 (m, Ph)
3		204.3[c]	
4	286.0	206.6 (2), 201.1, 200.7, 195.8, 194.6, 191.3 (2), 189.0, 184.6	47.85 (CH_3)
5a	283.6	209.3 (2), 206.8 (d, J_{PC} = 7.04), 202.4, 198.4 (dd, J_{PC} = 5.28, J_{CH} = 14.1), 197.2 (d, J_{CH} = 12.3), 193.6, 192.1 (d, J_{PC} = 12.31), 190.6	128-134 (m, Ph), 47.46 (s, CH_3)
6a	301.9	201.8, 200.6, 200.0, 199.6, 198.9, 197.8, 195.1, 194.0, 184.3, 176.2	57.3 (s, CH_2), 8.74 (s, CH_3)
6b	300.9	201.6, 200.7, 199.6, 199.2, 198.3, 196.6, 194.0, 184.0, 175.9	57.5 (s, CH_2), 8.53 (s, CH_3)
7a	299.0	205.5 (d, J_{PC} = 5.28), 203.5, 203.1 (d, J_{PC} = 3.51), 202.2, 200.7 (d, J_{PC} = 2.48), 199.2, 196.8, 195.1 (d, J_{PC} = 17.59), 184.9	128-134 (m, Ph), 56.98 (s, CH_2), 8.51 (s, CH_3)
7d	301.7	203.8, 203.4 (d, J_{PC} = 8.8), 202.2, 201.5 (d, J_{PC} = 7.0), 200.9 (d, J_{PC} = 5.3), 199.4, 197.8, 196.0 (d, J_{PC} = 24.6), 184.9	56.9 (s, CH_2), 52.6 (d, J_{PC} = 3.5), 8.90 (s, CH_3)
7e	300.9	203.7, 203.5 (d, J_{PC} = 9.2), 202.6, 201.3 (d, J_{PC} = 7.3), 200.9 (d, J_{PC} = 5.5), 198.5, 197.2, 195.3 (d, J_{PC} = 25.6), 185.0	57.3 (s, CH_2), 52.7 (d, J_{PC} = 3.7), 9.35 (s, CH_3)

[a] In ppm, relative to Me_4Si (relative intensity 1 unless otherwise noted); coupling constants in Hz. [b] Solvent $CDCl_3$ with $Cr(acac)_3$ (0.05 M) added as a paramagnetic relaxation agent. [c] Only one resonance exhibited in the range −30 to +30 °C. [d] Resonances marked with an asterisk are those coalescing at −45 °C (see text).

Table IV. ^{13}C NMR Data for Dinuclear Derivatives[a,b]

compd	O=C(Et)	CO and other
8	288.1 (2)	203.1 (2), 200.4 (2), 194.7, 180.1, 55.4 (CH_2), 8.27 (CH_3)
9a	287.2 (2)	208.2 (2) (J_{PC} = 3.52), 203.1, 195.7 (2) (J_{PC} = 7.04), 128-134 (m, PPh), 55.73 (CH_2), 8.12 (CH_3)
9b	289.1 (2) (J_{PC} = 3.52)	207.1 (2) (J_{PC} = 7.04), 203.5 (2) (J_{PC} = 3.52), 195.4 (J_{PC} = 29.9)

[a] In ppm relative to Me_4Si (relative intensity 1 unless otherwise noted); coupling constants in Hz. [b] Solvent $CDCl_3$ with $Cr(acac)_3$ (0.05 M) added as a paramagnetic relaxation agent.

the remaining four carbonyl groups. No enrichment is observed for the acyl group, over a period of 8 h.

For **8** specific initial enrichment is observed for the two resonances a and c, Figure 6 and Figure 9 (supplementary material). The enrichment subsequently equilibrates into the resonances of the remaining CO groups, but not to the acyl groups.

Discussion

Syntheses and ^{13}CO Enrichment. Working under mild conditions, we observe almost exclusive monosubstitution of the cluster derivatives. In the acyl-bridged complexes this may well reflect an acceleration of substitution by the oxygen of the acyl group as noted by the Darensbourgs and co-workers in carboxylato complexes.[5,7] Isolable monosubstituted products thus result owing to specific site activation introduced by the bridging acyl group. The same activation must be responsible for the ease of ^{13}C substitution that is observed (see further comments about specific site enrichment and subsequent equilibration discussed below).

By contrast, the monosubstituted products of halogen-bridged derivatives are somewhat surprising in view of earlier reports. Exclusive disubstitution is reported for $Ru_3\{\mu\text{-}NO\}_2(CO)_8L_2$, L = PPh_3, $P(Me)Ph_2$,[8] and for $Os_3\{\mu\text{-}Cl\}_2(CO)_8L_2$, L = PPh_3,[9] while mixtures of mono- and disubstituted products are reported for $Os_3\{\mu\text{-}H,\mu\text{-}SPh\}(CO)_8L_2$, L = PEt_3, $P(Me)Ph_2$.[10] For the triosmium complexes substitutions

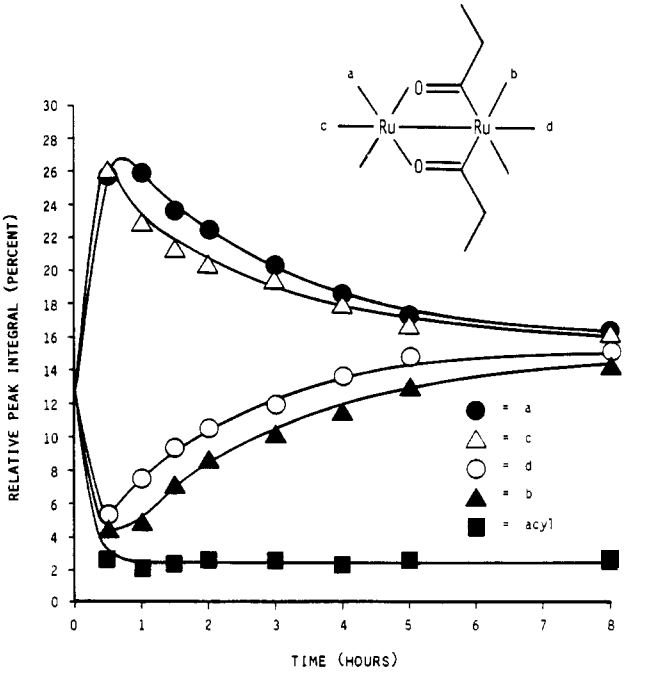

Figure 7. Site-specific enrichment in **8** and internal equilibration throughout the population of terminally bonded carbonyl groups. See caption to Figure 6 and text for further details.

were carried out in refluxing benzene; it is not known whether monosubstituted derivatives could have been isolated at lower reaction temperatures. A monosubstituted complex is observed but not isolated in kinetic studies of the reaction of $Ru_3\{\mu\text{-}NO\}_2(CO)_{10}$ with ligands at 22 °C, $t_{1/2}$ ca. 1.9 h.[8] Thus the reactions we report here at 25 °C must reflect a different ratio of rate constants for the first substitution as compared to those for subsequent substitutions. In this connection we should also call attention to the exclusive formation of $Ru_3(CO)_9L_3$, L = PPh_3, in the range 40–60 °C in the pioneering work of Candlin and Shortland,[11] which results from rapid subsequent substitutions on the initial product $Ru_3(CO)_{11}L$.

Assignments of ^{13}C NMR Spectra and the Position of the Phosphorus Ligand in Substituted Complexes. The spectrum

(7) Cf.: Darensbourg, D. J.; Rokicki, A.; Darensbourg, M. Y. *J. Am. Chem. Soc.* **1981**, *103*, 3223-3224.
(8) Norton, J. R.; Collman, J. P. *Inorg. Chem.* **1973**, *12*, 476-478.
(9) Deeming, A. J.; Johnson, B. F. G.; Lewis, J. *J. Chem. Soc. A* **1970**, 897-900.
(10) Deeming, A. J.; Johnson, B. F. G.; Lewis, J. J. *Chem. Soc. A* **1970**, 2517-2520.
(11) (a) Candlin, J. P.; Shortland, A. C. *J. Organomet. Chem.* **1969**, *16*, 289-299. (b) Use of sodium diphenylketyl in these reaction mixtures permits isolation of the monosubstituted derivatives in high yield. Cf.: Bruce, M. I.; Matisons, J. G.; Nicholson, B. K. *J. Organomet. Chem.* **1983**, *247*, 321-343.

of $Ru_3\{\mu\text{-}H,\mu\text{-}Cl\}(CO)_{10}$ (**1a**) (Figure 1 and Table III) is analogous in its intensity pattern to that reported for the corresponding triosmium complex.[12a] These patterns conform to the structure[3b,12b] and assignments indicated in Figure 1 and are derived in part by comparison with the spectrum of **2a**, discussed below. The lowest field resonances in both complexes are assigned to the axial carbonyl groups in agreement with previous work (on triosmium complexes).[13-16] This is supported by the appearance of satellites between the principal resonances, best seen in **2a** (upper scan, Figure 2). The satellites arise from the AB pattern of the *trans*-$^{13}CO_a$–Ru–$^{13}CO_b$ substituted species.[13] In connection with the assignments shown in Figure 1, it should be noted that coalescence is observed at 25 °C for resonances e, f, g, h, i, and j in **1a**.[3b]

The ^{13}C NMR spectrum of the triphenylphosphine-substituted complex **2a** (lower trace of Figure 1 and Table III) is consistent with a structure of C_1 symmetry. We can immediately rule out substitution of ligand at either positions a or b (see structural formula in Figure 1) since this would result in a structure of higher (C_s) symmetry. We return to this point later. The pattern of ^{31}P splitting (also identified in the top scan of Figure 2) suggests that the phosphorus atom is located cis to two carbonyl groups and trans to a third.

More specific information about the placement of the phosphorus ligand comes from signal e (lower scan, Figure 2); this resonance shows coupling to the bridging hydrogen atom as well as to phosphorus of the ligand. The observed coupling to μ-H is assigned as $J(\mu\text{-}^1H\text{–}Ru\text{–}^{13}CO, \text{trans})$; cis couplings are significantly lower in magnitude and are usually not observed. The magnitude of the trans coupling in our work ranges from 11.0 through 15.9 Hz (see Table III and Scheme I). This is comparable to what has been reported for edge-double-bridged complexes containing hydrogen as one or both of the bridging atoms; cf. 10.7 Hz for $Os_3\{\mu\text{-}H\}_2(CO)_{10}$[15] or values in the range 9.6–15 Hz for the derivatives $Os_3\{\mu\text{-}H,\mu\text{-}X\}(CO)_{10}$.[12]

The carbonyl group corresponding to resonance e is thus fixed in a position trans to μ-H; the phosphorus ligand must be in one or the other of the two positions cis to μ-H. *cis*-^1H–Ru–^{31}P coupling in our derivatives is in the range 4.8–10.3 Hz (Scheme I and Table II). This is comparable to values of $J(\mu\text{-}^1H\text{–}Os\text{–}^{31}P, \text{cis})$ found in $Os_3\{\mu\text{-}H\}_2(CO)_9L$ (Hz): 7.0, L = PPh_3; 6.5, L = PMe_2Ph;[17a] 6.9, L = PEt_3.[17b] These are well below values for $J(\mu\text{-}^1H\text{–}Os\text{–}^{31}P, \text{trans})$ found in the range 23–30 Hz for $Os_3\{\mu\text{-}H,\mu\text{-}SPh\}(CO)_8L_2$, L = PEt_3, $P(Me)Ph_2$.[10] The *cis*-^{31}P–Ru–^{13}CO coupling constants in the range 5.2–7.1 Hz (Schemes I and II and Table III) are comparable to values reported in the literature for such interactions.[13-15]

The phosphorus ligand is unambiguously placed at position g (Figure 1 or 2) by its larger coupling to an additional carbonyl group, the one in position trans across the metal–metal bond, i.e. ^{31}P–Ru–Ru–$^{13}CO_d$. This assignment is confirmed by similar features observed in $Ru_3\{\mu\text{-}H,\mu\text{-}O{=}CNMe_2\}(CO)_9P(OPh)_3$, in which the triphenyl phosphite ligand has been shown by X-ray structure determination to occupy the same position as assigned to the triphenylphosphine in **2a**.[1]

Similar coupling through the metal–metal bond, $J(^{31}P\text{–}Ru\text{–}Ru\text{–}^{13}CO_d, \text{trans})$, is observed for all compounds in this work with values ranging between 11.6 and 29.9 Hz (Schemes I and II and Tables III and IV). These may be compared to values for ^{31}P–Ir–Ir–^{13}C coupling in the range 14–33 Hz for the complexes $Ir_4(CO)_{12-x}L_x$.[18] We suggest that the $^{13}C\text{–}^{31}P$ coupling of 8.3 Hz reported (but not assigned) for the complex $Ru_3(CO)_8(NO)_2(PPh_3)_2$[5] may also represent this type of long-range coupling.

To finish discussion of the spectra in Figures 1 and 2, we assign resonance h as that arising from the second carbonyl group trans to the bridging hydrogen from the splitting observed in the lower scan of Figure 2. We note this resonance to be one of the three that disappear in the room-temperature spectrum due to stereochemical nonrigidity of the unique $Ru(CO)_3$ group on the double-bridged edge.

Parallel considerations apply to the spectra of $Ru_3\{\mu\text{-}H,\mu\text{-}O{=}C(Me)\}(CO)_{10}$ (**4**) and its phosphine-substituted derivative, **5a**, which undergo no exchange processes at room temperature (Figure 3). In **4**, the resonances of carbonyl groups a and b as well as c and d are found to be accidentally degenerate. By contrast, pairs of resonances e, h and f, i, degenerate in **1a**, are seen to be separated in **4**, arising from asymmetry due to the acyl bridging group. Assignments of resonances e and h of **5a** are confirmed through the proton-coupled spectrum (not shown here); doublet e appears as a quartet (2 × 2), and singlet h appears as a doublet (see Scheme I for the coupling constants). We exclude the phosphorus ligand from a position on the ruthenium atom to which the carbon of the acyl group is bonded by *lack* of $^{31}P\text{–}^{13}C$ coupling of this resonance in **5a** as well as in **7a,d,e** discussed next.

The ^{13}C NMR spectrum of $Ru_3\{\mu\text{-}Cl,\mu\text{-}O{=}C(Et)\}(CO)_9PPh_3$ (**7a**) is shown in Figure 4 (supplementary material). It is analogous to that discussed for **5a** above and fully consistent with the structure shown in Scheme II except that **7a,d,e** exhibit one additional, small coupling to phosphorus in a resonance as yet not assigned (Table III).

The ^{13}C NMR spectrum of $Ru_2\{\mu\text{-}O{=}C(Et)\}_2(CO)_5P(OMe)_3$ (**9b**) is given in Table IV and shown in Figure 5. Four resonances are observed in the carbonyl region. Each shows coupling to phosphorus: the doubly degenerate acyl carbon resonance, identified by its low-field chemical shift (289.1 ppm), exhibits a small but identical coupling (J_{PC} = 3.52 Hz) with that of a second resonance, also of relative intensity 2; a third signal shows a larger coupling (J_{PC} = 7.04 Hz), and the remaining signal of relative intensity 1 exhibits a large coupling (J_{PC} = 29.9 Hz). These data are fully consistent with placement of phosphorus ligand at the site on the ruthenium atom bonded to the oxygen atoms of the two acyl groups, trans to the ruthenium–ruthenium bond.

Site-Specific Enrichment and Fluxional Processes. In the two parent complexes **6a** and **8** (which do not exhibit fluxional behavior on the NMR time scale) we observe site-specific enrichment under ^{13}CO exchange (see Results). In **6a** all three carbonyl groups on the ruthenium atom attached to the oxygen of the acyl group as well as one of the carbonyl groups of the other ruthenium on the doubly-bridged edge (h) are seen to be instantaneously enriched with ^{13}CO. Within 2 h, this enrichment spreads to the resonances of the remaining carbonyl groups (i and j) on the double-bridged edge, followed by equilibration into the resonances of the remote $Ru(CO)_4$ group over an additional 6 h.

In **8**, immediate enrichment is also observed in the resonances of the carbonyl groups located on the ruthenium atom attached to the oxygen atoms of the two bridging acyl groups (see Results).

(12) (a) Bryan, E. G.; Forster, A.; Johnson, B. F. G.; Lewis, J.; Matheson, T. W. *J. Chem. Soc., Dalton Trans.* **1978**, 196–198. (b) For the structure of $Os_3\{\mu\text{-}H,\mu\text{-}Br\}(CO)_{10}$ see: Churchill, M. R.; Lashewycz, R. A. *Inorg. Chem.* **1979**, *18*, 3261–3265; (c) For the structure of $Ru_3\{\mu\text{-}H,\mu\text{-}Br\}(CO)_{10}$ see ref 3b.
(13) Keister, J. B.; Shapley, J. R. *Inorg. Chem.* **1982**, *21*, 3304–3310.
(14) Johnson, B. F. G.; Lewis, J.; Reichert, B. E.; Schorpp, K. T. *J. Chem. Soc., Dalton Trans* **1976**, 1403–1404.
(15) Aime, S.; Osella, D.; Milone, L.; Rosenberg, E. *J. Organomet. Chem.* **1981**, *213*, 207–213.
(16) Willis, A. C.; Einstein, F. W. B.; Ramadan, R. M.; Pomeroy, R. K. *Organometallics* **1983**, *2*, 935–936.
(17) (a) Deeming, A. J.; Hasso, S. *J. Organomet. Chem.* **1975**, *88*, C21–C23. (b) Bryan, E. G.; Jackson, W. G.; Johnson, B. F. G.; Kelland, J. W.; Lewis, J.; Schorpp, K. T. *J. Organomet. Chem.* **1976**, *108*, 385–391.
(18) Stuntz, G. F.; Shapley, J. R. *J. Am. Chem. Soc.* **1977**, *99*, 607–609.

The relative intensity of the acyl group resonances in both **6a** and **8** remains constant following a drop in their relative intensity immediately after enrichment at other sites. This indicates that these groups do not participate in exchange over the 8-h period of our experiments. The curves in Figures 6 and 7 do not fit any simple kinetic expression; however, the half-life for redistribution in all carbonyl groups except for the acyl group may be graphically estimated to be between 1 and 2 h for both derivatives.

Fluxional Behavior on the NMR Time Scale. This is observed in only four of the derivatives studied, namely **3** and **2a–c**. In $Ru_3\{\mu\text{-}H,\mu_3\text{-}I\}(CO)_8PPh_3$ (**3**) we see the averaged spectrum of one signal down to −30 °C. This must involve delocalized migration over the whole cluster unit[19] and is similar to what is observed for the parent complex $Ru_3\{\mu\text{-}H,\mu_3\text{-}I\}(CO)_9$, which exhibits one resonance down to −80 °C.[3b] Capped triruthenium complexes with two or three bridging hydrogen atoms exhibit higher barriers to fluxional processes: $Ru_3\{\mu\text{-}H\}_2\{\mu_3\text{-}S\}(CO)_9$[20] exhibits one resonance above 50 °C, two signals at 0 °C, and the limiting spectrum of five resonances at −108 °C; $Ru_3\{\mu\text{-}H\}_3\{\mu_3\text{-}CCH_3\}(CO)_9$ exhibits the limiting spectrum of two resonances over the entire range −60 to +90 °C.[20]

For $Ru_3\{\mu\text{-}H,\mu\text{-}Cl\}(CO)_9PPh_3$ (**2a**) three of the signals seen at −50 °C are absent at 35 °C (upper scan, Figure 2). We have assigned these as the three carbonyl groups h, i, and j, also observed to exchange rapidly with each other in the parent complex **1a**.[3b] Similar fluxionality is observed for resonances h, i, and j in **2b** and **2c**. Resonances e, f, and g, also observed to undergo rapid exchange in **1a**,[3b] are locked into place in **2a–c** by substitution of phosphorus ligand at position g (see structural diagram, top of Figure 1).

^{1}H NMR. For compounds **2a–c** and **3**, resonances are uniformly at lower field (range −13.0 to −16.1 ppm) than those of the corresponding unsubstituted derivatives (range −14.16 to −17.7 ppm). This follows similar observations in studies cited earlier.[17] ^{31}P–^{1}H coupling constants have been discussed above.

Compounds **7a–f** and **9a–c** exhibit an ABX_3 pattern for the diastereotopic CH_2 protons in the μ-propionyl group.[4b]

^{31}P{^{1}H} NMR. These resonances for triphenylphosphine-substituted derivatives lie in the range 14.3–37.5 ppm (relative to 85% H_3PO_4) while those for the trimethyl or triphenyl phosphite complexes lie at higher field (range 116–152 ppm). ^{31}P–^{13}C coupling constants discussed above are those observed in the ^{13}C NMR spectra.

IR. The six maxima observed in the carbonyl region of the complexes **2a–c** may be compared with those reported for the structurally similar triosmium complex $Os_3(\mu\text{-}H)_2(CO)_9PPh_3$.[17] The patterns are similar except that the latter contains one additional maximum (2004 m cm^{-1}) as is common in comparisons between ruthenium and osmium analogues (paralleling spectra of the parent carbonyls in which the maxima of four medium or strong bands are seen for $Os_3(CO)_{12}$ but only three are observed for $Ru_3(CO)_{12}$).[21] Selected spectra are offered as supplementary material.

Experimental Section

General Considerations. Substitution reactions were performed under nitrogen in standard Schlenk-type glassware as a matter of routine although we also found that exposure to air has no observable deleterious effect on the complexes described in this work. Solvents were degassed by bubbling nitrogen through them for 5–10 min. All chromatographic separations in this work were performed on Silica Gel 60 (70–230 mesh, E. Merck, Darmstadt, West Germany-MC/B Manufacturing Chemists, Cincinnati, OH 45212) using a column 2.5 cm^2 × 25 cm. Analytical determinations were carried out by Schwartzkopf Microanalytical Laboratories, Woodside, NY 11377.

Solvents and Reagents. These were of commercial reagent grade and used without further purification. $Ru_3(CO)_{12}$ was prepared[22] from $RuCl_3\cdot 3H_2O$ obtained from Strem Chemicals, Inc. ^{13}C-labeled CO (99%) was obtained from Isotec, Inc. Starting materials identified below were prepared from published methods: **1a–c**,[3b] **4** and **8**.[4b]

Instrumentation. Infrared spectra were obtained on a Nicolet MX-1 Fourier transform spectrometer using cells equipped with CaF_2 windows. ^{1}H NMR spectra were run at 35 °C on a Bruker WM-200 spectrometer and are referenced to tetramethylsilane. ^{13}C NMR spectra were obtained in the temperatue range −80 to +40 °C on a JEOL FX90Q spectrometer, referenced to tetramethylsilane. ^{31}P NMR spectra were obtained on the same instrument, referenced to 85% phosphoric acid.

Reaction of $Ru_3\{\mu\text{-}H,\mu\text{-}X\}(CO)_{10}$, X = Cl (1a), Br (1b), I (1c), with PPh_3. The procedure for **1a** given here applies to all three of the cited compounds. Solutions of **1a** (150 mg, 0.242 mmol) in 150 mL of hexane and of PPh_3 (63.5 mg, 0.242 mmol) in 5 mL of hexane are combined at room temperature in a 200-mL Schlenk flask connected to a mineral oil bubbler under a nitrogen atmosphere. The solution turns from orange to red, and the reaction is complete within 10 min as monitored by the disappearance of the characteristic CO stretching frequencies of **1a** in the region 1500–2250 cm^{-1} in the infrared. The volume of solvent is then reduced under vacuum to 5 mL and the resulting solution chromatographed with petroleum ether as eluant. The first, fast-moving band is unreacted starting material followed by a slow-moving red band, $Ru_3\{\mu\text{-}H,\mu\text{-}Cl\}(CO)_9PPh_3$ (**2a**). A third orange band elutes with 10/90 CH_2Cl_2/petroleum ether and corresponds to the disubstituted derivative (2080 s, 2031 m, 2008 vs, 1984 w, 1963 w cm^{-1}). Solvent from the solution containing the second fraction is removed under vacuum, and ca. 3 mL of degassed spectral grade pentane is used to dissolve the residue. This solution is then cooled to −20 °C to give deep red crystals of **2a** (124 mg, 0.145 mmol, 60%). The yields for **2b** and **2c** are both 55%. Anal. Calcd for $Ru_3\{\mu\text{-}H,\mu\text{-}Cl\}(CO)_9PPh_3$ (**2a**), $C_{27}H_{16}O_9ClPRu_3$: C, 37.97; H, 1.89; P, 3.63; Cl, 4.15. Found: C, 37.67; H, 1.97; P, 3.69; Cl, 4.21.

Complex **2c** slowly loses CO to form $Ru_3\{\mu\text{-}H,\mu_3\text{-}I\}(CO)_8PPh_3$ (**3**). Conversion to **3** is expedited by dissolving **2c** and then removing solvent under vacuum; this is repeated twice. This transformation is reversed under 1 atm of CO. **3** is separated by column chromatography, eluting as an orange band following the red band of **2c**. Crystallization from pentane yields red crystals of **3** in 40% yeild.

Reaction of $Ru_3\{\mu\text{-}H,\mu\text{-}O{=}C(Me)\}(CO)_{10}$ (4) with PPh_3 or $P(OMe)_3$. Solutions of **4** (329 mg, 0.524 mmol) in 400 mL of hexane and PPh_3 (138 mg, 0.524 mmol) in 10 mL of hexane are combined at room temperature under a nitrogen atmosphere. The initial orange color gradually darkens as substitution ensues. After 4 h, solvent volume is reduced to 5 mL and the solution chromatographed on a silica gel column with petroleum ether as eluant. The first, fast-moving, orange-yellow band is $Ru_3(CO)_{12}$. This is followed by a small amount of $H_2Ru_4(CO)_{13}$ (red band). The third fraction is unreacted, bright yellow **4** (82 mg). A fourth, dark red band, corresponding to $Ru_3(CO)_{11}PPh_3$, elutes with 20/80 CH_2Cl_2/petroleum ether and is followed by a light, red-orange band, **5a**. The solvent from the eluate containing **5a** is removed under vacuum, and ca. 3 mL of degassed spectral grade pentane is used to dissolve the residue. This solution is cooled to −20 °C, yielding dark red crystals of **5a** (162 mg, 0.188 mmol, 48% based on reacted **4**). Anal. Calcd for $Ru_3\{\mu\text{-}H,\mu\text{-}O{=}CMe\}(CO)_9PPh_3$ (**5a**), $C_{29}H_{19}O_{10}PRu_3$: C, 40.43; H, 2.22; P, 3.59. Found: C, 40.56; H, 2.33; P, 3.58.

The reaction of **4** with $P(OMe)_3$ requires a 20-fold excess of phosphite for substitution to occur and gives a lower yield of monosubstituted product; addition of 1 equiv of $P(OMe)_3$ to **4** in hexane at room temperature is found to result in no reaction observable by IR after 24 h. To a solution of **4** (573 mg, 0.91 mmol/500 mL of hexane) is added a solution of $P(OMe)_3$ (18.2 mmol, 10% by weight in hexane), and the mixture stirred until disappearance of carbonyl IR absorptions of **4** in the region 2250–1500 cm^{-1}, ca. 1 h. Column chromatography of the reaction mixture resolves four fractions. The

(19) Johnson, B. F. G.; Benfield, R. E. In "Transition Metal Clusters"; Johnson, B. F. G., Ed.; Wiley-Interscience: New York, 1980; Chapter VII.

(20) Forster, A.; Johnson, B. F. G.; Lewis, J.; Matheson, T. W. *J. Organomet. Chem.* **1976**, *104*, 225.

(21) Battiston, G. A.; Bor, G.; Dietler, U. K.; Kettle, S. F. A.; Rossetti, R.; Sbrignadello, G.; Stanghellini, P. L. *Inorg. Chem.* **1980**, *19*, 1961.

(22) (a) Bruce, M. I. *J. Chem. Soc., Dalton Trans.* **1983**, 2365. (b) Jensen, C. M.; Jones, N. L. *Inorg. Synth.*, in press.

first is $Ru_3(CO)_{12}$; the second elutes with 15/85 CH_2Cl_2/petroleum ether, as an orange band. This is **5b**. Unreacted **4**, 10 mg, follows next; a faint red band with a simple infrared pattern (2085 w, 2049 w, 2030 s, 2005 vs, 1984 w cm^{-1}) follows **4**. A fourth, deep red fraction identified as $Ru_3(CO)_{11}P(OMe)_3$ is last. The solvent from the eluate containing **5b** is removed under vacuum and the residue dissolved in ca. 5 mL of degassed spectral grade pentane. Cooling to −20 °C produces deep red crystals of **5b** (100 mg, 0.14 mmol, 15%).

Reaction of $Ru_3\{\mu$-X,μ-O=C(Et)$\}(CO)_{10}$, X = Cl (6a), Br (6b), I (6c), with PPh_3 or $P(OMe)_3$. The procedure for the reaction of PPh_3 with **6a** is given here; the same may be used for the synthesis of the other derivatives cited in Scheme II. Solutions of **6a** (80 mg, 0.13 mmol/100 mL of hexane) and PPh_3 (34 mg, 0.13 mmol/5 mL of hexane) are combined at room temperature under nitrogen. This is accompanied by an instantaneous color change from red to yellow; the reaction is complete in less than 1 min as monitored by IR. The solution is reduced in volume under vacuum to 5 mL and chromatographed on a silica gel column using petroleum ether as eluant. $Ru_3\{\mu$-Cl,μ-O=C(Et)$\}(CO)_9PPh_3$ (**7a**) elutes with 10/90 CH_2Cl_2/petroleum ether as a bright yellow fraction. Product is crystallized from pentane to give yellow crystals of **7a** (116 mg, 130 mmol, 98%).

By similar procedures using $P(OMe)_3$ instead of PPh_3, $P(OMe)_3$-substituted products **7d–f** are obtained. Anal. Calcd for $Ru_3\{\mu$-Cl,μ-O=C(Et)$\}(CO)_9P(OMe)_3$ (**7d**), $C_{15}H_{14}O_{13}ClPRu_3$: C, 23.34; H, 1.83; P, 4.01; Cl, 4.59. Found: C, 23.73; H, 2.08; P, 4.01; Cl, 4.23.

Reaction of $Ru_2\{\mu$-O=C(Et)$\}_2(CO)_6$ (8) with PPh_3, $P(OMe)_3$, and $P(OPh)_3$. To a solution of **8** (100 mg, 0.206 mmol/100 mL of hexane) is added 1 equiv of the desired phosphine or phosphite. Reaction is complete within 1 min as monitored by IR. The solution is reduced in volume and chromatographed on a silica gel column. The substituted product elutes with 10/90 CH_2Cl_2/petroleum ether as a faint yellow band. No other fractions are observed. Products **9a–c** are obtained as oils in essentially 100% yield. Anal. Calcd for $Ru_2\{\mu$-O=C(Et)$\}_2(CO)_5PPh_3$ (**9a**), $C_{29}H_{25}O_7PRu_2$: C, 48.47; H, 3.51; P, 4.31. Found: C, 48.43; H, 3.60; P, 4.38.

^{13}CO Exchange. Quantities of **1a–c**, **4**, **6a–c**, and **8** were enriched with ^{13}CO to approximately 30% by the following procedure. A solution of the appropriate derivative in hexane is placed in a 5-mm NMR tube leaving a gas volume of approximately 2 mL. ^{13}CO gas (99%) is introduced, and the contents of the tube are shaken vigorously for 30 s. Phosphine or phosphite is then introduced as described in the foregoing sections.

Study of Time Dependence of ^{13}C Enrichment in 6a and 8. Solutions of ca. 0.30 mmol of these derivatives and $Cr(acac)_3$ (20 mg) in 0.5 mL of CDCl are each placed in a 5-mm NMR tube. A series of 10 spectra each collected over a 30-min period at 32 °C is obtained of the unenriched samples to determine the reproducibility of the integrals of the ^{13}C resonances of the carbonyl groups. The area under each of the peaks is determined by the method of cutting and weighing: reproducibility, σ = 0.8%. The last spectrum of the series is taken to represent the spectrum of the unenriched sample at t = 0 in the sequence described below.

The same procedure described above is followed for ^{13}CO exchange; introduction of ^{13}CO is taken to be t = 0. A spectrum is taken to t = 30 min after first exposure to ^{13}CO. At this point, the solution is purged of CO by bubbling through N_2 for 30 s. Additional spectra are recorded at 30-min intervals for a period of 8 h and then after 1-h periods for an additional 4 h.

Spectra were then plotted, and the area under each of the resonances was determined by the cut and weigh technique. The relative areas in percent of the total are normalized and plotted as shown in Figure 6 (supplementary material) for **6a** or in Figure 9 (supplementary material) for **8**.

Summary

In all three types of trinuclear complexes studied here the substitution of a carbonyl group by a phosphorus ligand has taken place on a ruthenium atom of the double-bridged edge. Where an acyl group is one of the bridging groups, the substitution occurs on the ruthenium atom to which the oxygen atom of the acyl group is bonded. In the two derivatives $Ru_3\{\mu$-Cl,μ-O=C(Et)$\}(CO)_{10}$ and $Ru_2\{\mu$-O=C(Et)$\}_2(CO)_6$, initial ^{13}CO enrichment is seen to be site specific, in all three carbonyl groups on the ruthenium to which the oxygen atom of the acyl group is attached. In the former, a carbonyl group on the second of the ruthenium atoms of the doubly bridged edge is also involved in the initial enrichment.

Acknowledgment. This work was supported by a grant from the National Science Foundation (Grant No. CHE-79-08406). The Bruker WM-200 spectrometer was purchased with support from NSF Grant No. CHE-76-05926.

Registry No. **1a**, 80800-55-1; **1b**, 80800-54-0; **1c**, 80800-56-2; **2a**, 93403-41-9; **2b**, 93403-42-0; **2c**, 93403-43-1; **3**, 93403-44-2; **4**, 80800-53-9; **5a**, 93403-45-3; **5b**, 93403-46-4; **6a**, 85220-76-4; **6b**, 85220-77-5; **6c**, 88403-89-8; **7a**, 93425-37-7; **7b**, 93403-47-5; **7c**, 93403-48-6; **7d**, 93403-49-7; **7e**, 93403-50-0; **7f**, 93403-51-1; **8**, 85220-87-7; **9a**, 93403-52-2; **9b**, 93403-53-3; **9c**, 93403-54-4; $Ru_3\{\mu$-H,μ-Cl$\}(CO)_8(PPh_3)_2$, 93403-55-5; $H_2Ru_4(CO)_{13}$, 21077-76-9; $Ru_3(CO)_{12}$, 15243-33-1; $Ru_3(CO)_{11}PPh_3$, 38686-52-1; $Ru_3(CO)_{11}P(OMe)_3$, 82532-25-0.

Supplementary Material Available: $^{13}C\{^1H\}$ spectra in the carbonyl region for **6a**, **7a**, and **8** (Figures 4, 8, and 9) and infrared spectra in the carbonyl region for compounds **2a**, **3**, **4**, **5a**, **7a**, **7d**, and **9c** (6 pages). Ordering information is given on any current masthead page.